Published OnlineFirst September 11, 2015; DOI: 10.1158/0008-5472.CAN-14-3603

Molecular and Cellular Pathobiology

Cancer Research

Radioprotection of *IDH1*-Mutated Cancer Cells by the IDH1-Mutant Inhibitor AGI-5198

Remco J. Molenaar[1], Dennis Botman[1], Myrthe A. Smits[1], Vashendriya V. Hira[1], Sanne A. van Lith[2], Jan Stap[1], Peter Henneman[3], Mohammed Khurshed[1], Krissie Lenting[2], Adri N. Mul[3], Dionysia Dimitrakopoulou[1], Cornelis M. van Drunen[4], Ron A. Hoebe[1], Tomas Radivoyevitch[5], Johanna W. Wilmink[6], Jaroslaw P. Maciejewski[7], W. Peter Vandertop[8,9], William P. Leenders[2], Fonnet E. Bleeker[3], and Cornelis J. van Noorden[1]

Abstract

Isocitrate dehydrogenase 1 (*IDH1*) is mutated in various types of human cancer to IDH1^{R132H}, a structural alteration that leads to catalysis of α-ketoglutarate to the oncometabolite *D*-2-hydroxyglutarate. In this study, we present evidence that small-molecule inhibitors of IDH1^{R132H} that are being developed for cancer therapy may pose risks with coadministration of radiotherapy. Cancer cells heterozygous for the IDH1^{R132H} mutation exhibited less IDH-mediated production of NADPH, such that after exposure to ionizing radiation (IR), there were higher levels of reactive oxygen species, DNA double-strand breaks, and cell death compared with *IDH1* wild-type cells. These effects were reversed by the IDH1^{R132H} inhibitor AGI-5198. Exposure of *IDH1* wild-type cells to *D*-2-hydroxyglutarate was sufficient to reduce IDH-mediated NADPH production and increase IR sensitivity. Mechanistic investigations revealed that the radiosensitivity of heterozygous cells was independent of the well-described DNA hypermethylation phenotype in *IDH1*-mutated cancers. Thus, our results argue that altered oxidative stress responses are a plausible mechanism to understand the radiosensitivity of *IDH1*-mutated cancer cells. Further, they offer an explanation for the relatively longer survival of patients with *IDH1*-mutated tumors, and they imply that administration of IDH1^{R132H} inhibitors in these patients may limit irradiation efficacy in this setting. *Cancer Res; 75(22); 4790–802. ©2015 AACR.*

Introduction

IDH1 and lDH2 are homodimeric enzymes that reversibly convert isocitrate to α-ketoglutarate (αKG) with concomitant reduction of $NADP^+$ to NADPH in the cytoplasm and mitochondria, respectively (1). Somatic heterozygous hotspot mutations in *IDH1/2* (*IDH*^{MT}) are observed in substantial percentages of various tumor types, such as glioma (80%), acute myeloid leukemia (AML, 20%), cholangiocarcinoma (20%), chondrosarcoma (60%), and others (1).

IDH^{MT} cause metabolic changes in cancer (2). All *IDH*^{MT}, of which *IDH1*^{R132H} is the most prevalent in glioma, cause loss of enzymatic wild-type IDH (IDH^{WT}) function (3–5). In addition, IDH^{MT} have a neo-enzymatic (gain of function) activity: it converts αKG and NADPH to *D*-2-hydroxyglutarate (*D*-2HG) and $NADP^+$. *D*-2HG is an oncometabolite that is present in trace amounts in *IDH*^{WT} cells but accumulates to levels up to 50 mmol/L in *IDH*^{MT} cancers (6). Because of the chemical similarities between *D*-2HG and αKG, *D*-2HG competitively inhibits αKG-dependent dioxygenases, such as ten-eleven translocation factor 2 (TET2) and JmjC-domain containing histone lysine demethylases (JHKDM; refs. 7, 8). This results in a CpG island methylation phenotype (CIMP), which alters gene expression and induces malignant transformation (9).

Patients with *IDH*^{MT} glioma and cholangiocarcinoma have up to 3-fold longer median overall survival times than *IDH*^{WT} counterparts (3, 5, 10–12). Altered patient survival caused by differences in *IDH1*^{MT} versus *IDH1*^{WT} tumor biology may be on the level of intrinsically reduced malignancy, and/or altered responses to therapy. We previously showed in human glioblastoma samples that *IDH1*^{MT} are associated with a 38% decrease in IDH-mediated NADPH production capacity (5). NADPH is the most important source of reducing power for cellular detoxification of oxidants, because it is an essential cofactor for the regeneration of reduced glutathione (GSH) from oxidized glutathione (GSSG) by glutathione reductase. Therefore, we and others proposed that altered redox responses result in increased responses to therapy in

[1]Department of Cell Biology and Histology, Academic Medical Center, University of Amsterdam, Amsterdam, the Netherlands. [2]Department of Pathology, Radboud University Medical Center, Nijmegen, the Netherlands. [3]Department of Clinical Genetics, Academic Medical Center, University of Amsterdam, Amsterdam, the Netherlands. [4]Department of Otorhinolaryngology, Academic Medical Center, University of Amsterdam, Amsterdam, the Netherlands. [5]Department of Quantitative Health Sciences, Lerner Research Institute, Cleveland Clinic, Cleveland, Ohio. [6]Department of Medical Oncology, Academic Medical Center, University of Amsterdam, Amsterdam, the Netherlands. [7]Department of Translational Hematology and Oncology Research, Taussig Cancer Institute, Cleveland Clinic, Cleveland, Ohio. [8]Department of Neurosurgery, Academic Medical Center, University of Amsterdam, Amsterdam, the Netherlands. [9]Department of Neurosurgery, VU Medical Center, Amsterdam, the Netherlands.

Note: Supplementary data for this article are available at Cancer Research Online (http://cancerres.aacrjournals.org/).

Corresponding Author: R.J. Molenaar, Academic Medical Center, University of Amsterdam, Meibergdreef 15, 1105AZ Amsterdam, the Netherlands. Phone: 31-20-5668587; Fax: 31-20-5669691; E-mail: r.j.molenaar@amc.nl

doi: 10.1158/0008-5472.CAN-14-3603

Published OnlineFirst September 11, 2015; DOI: 10.1158/0008-5472.CAN-14-3603

IDH1^{MT} cancers (1, 13–15). This hypothesis is supported by *in vitro* studies, showing that overexpression of IDH1^{R132H} sensitizes glioma cells to ionizing radiation (IR) or chemotherapy with carmustine (BCNU), *cis*-diaminedichloroplatinum (CDDP), or temozolomide (15–17). In addition, there is clinical evidence that *IDH1*^{MT} sensitize glioma to a procarbazine, lomustine (CCNU), and vincristine (PCV) regimen (18) and sensitize glioblastoma to a combination of IR and temozolomide (19).

IDH^{MT} are early events in the formation of glioma (20), chondrosarcoma (21), and cholangiocarcinoma (22), which makes *IDH*^{MT} attractive therapeutic targets. Inhibitors of IDH1^{MT} and IDH2^{MT} were recently developed (23–27). Clinical trials of the IDH1^{R132H} inhibitor AGI-5198 (ClinicalTrials.gov NCT02073994) are in progress in solid tumors. AGI-5198 inhibits IDH1^{R132H} neoenzymatic activity, which decreases *D*-2HG production in *IDH1*^{MT} cells, and thus inhibits carcinogenesis (23). However, better prognosis of patients with established *IDH*^{MT} glioma or cholangiocarcinoma (which are past the carcinogenesis stage) may be related to increased anticancer therapy responses by virtue of increased oxidative stress in these tumors due to a lower NADPH production capacity. Thus, we argued that inhibition of IDH^{MT} decreases this stress and consequently increases cancer cell survival (1, 2).

The aim of the present study is to provide *in vitro* evidence that the prolonged overall survival of glioma patients with *IDH1*^{MT} tumors is caused by increases in oxidative stress, and in particular, reduced NADPH production capacity. We investigated whether this stress affects the response to IR and metformin. Moreover, we studied whether the IDH1^{R132H} inhibitor AGI-5198 blocks this metabolic stress, thus interfering with the survival-prolonging properties of *IDH1*^{MT}.

Materials and Methods

Cell lines

HCT116 *IDH1*$^{WT/R132H}$ knock-in cells, generated by AAV targeting technology GENESIS (28), were kindly provided by Horizon Discovery Ltd. HT1080 chondrosarcoma cells were a kind gift of Dr. Hamann (Department of Experimental Immunology, AMC, University of Amsterdam). U251 and LN229 glioblastoma cells were stably transduced using lentiviral constructs encoding for IDH1^{WT} or IDH1^{R132H} as described earlier (29). Constructs contain a C-terminal biotin acceptor peptide and a HIS-tag, which allows distinction from endogenous IDH1^{WT} by molecular weight. IDH1^{WT} and IDH1^{R132H} expression was analyzed by Western blotting using a pan-IDH1 antibody (HPA0352428, Sigma-Aldrich) and a specific antibody recognizing IDH1^{R132H} (30). Western blots were analyzed using a Li-Cor Odyssey system (Li-Cor Biotechnology).

lDH1$^{WT/R132H}$ and *lDH1*$^{WT/WT}$ HCT116 cells were cultured in McCoy's 5A medium (Gibco; Life Technologies; Thermo Fisher Scientific) in 5% CO_2 at 37°C. U251, LN229, and HT1080 cells were cultured in 5% CO_2, 5% CO_2, and 10% CO_2, respectively, at 37°C in complete DMEM (Gibco). All media were supplemented with 10% FBS (HyClone; Thermo Fisher Scientific), 100 units/mL penicillin, and 100 μg/mL streptomycin (both Gibco).

Reagents

AGI-5198 was purchased from MedChemExpress; *L*-2HG, *D*-2HG, αKG, coenzyme A, thiamine pyrophosphate, and *N*-acetyl cysteine (NAC) were purchased from Sigma-Aldrich. Metformin was purchased from BioConnect.

Enzyme activity measurements

Cells were cultured in the presence of 200 to 800 nmol/L AGI-5198 or solvent only (DMSO, final concentration $\leq$ 0.5%) and subsequently trypsinized and centrifuged onto microscopy slides using a cytocentrifuge (Cytospin 4 Cytocentrifuge, Shandon, Thermo Fisher Scientific) at 20 rcf for 5 minutes at room temperature. Cytospins were air-dried for 1 day and subsequently stained using metabolic mapping to visualize NAD^+-dependent or $NADP^+$-dependent activities of IDH [EC numbers 1.1.1.41 (IDH3) and 1.1.1.42 (IDH1/2), respectively], NAD^+-dependent activity of αKG dehydrogenase (αKGDH; EC number 1.2.4.2), or $NADP^+$-dependent activity of glucose-6-phosphate dehydrogenase (G6PD; EC number 1.1.1.49). Enzyme activity experiments were conducted and analyzed as described previously (31, 32). We used nitrotetrazolium blue chloride (NBT; Sigma-Aldrich) in the enzyme reaction medium and a 585-nm monochromatic filter to exclusively record formazan produced from NBT. Incubation with substrate and cofactors was performed at 37°C for 60 minutes to detect $NADP^+$-dependent or NAD^+-dependent IDH activity (30 minutes for tissue), 60 minutes to detect NAD^+-dependent αKGDH activity, and 10 minutes to detect $NADP^+$-dependent G6PD activity. Control reactions were performed in the absence of substrate but in the presence of cofactors to control for nonspecific enzyme activity staining (31, 32). Enzyme activity measurements of cells overexpressing IDH1^{WT} or IDH1^{R132H} were normalized to enzyme activity measurements of parental cells by correcting for relative pan-IDH1 expression levels of cells, as determined by Western blotting.

We used supraphysiological substrate concentrations (up to 30 mmol/L) because the viscous 18% polyvinyl alcohol-containing enzyme reaction medium does not allow sufficient substrate diffusion at low concentrations. Thus, the determined enzyme activities do not reflect the *in vivo* situation at a given substrate concentration but are suitable for intraexperimental comparisons (31). *D*-2HG and *L*-2HG inhibition experiments were performed in the presence of 1 mmol/L isocitrate or 3 mmol/L αKG and 30 mmol/L *D*-2HG or 30 mmol/L *L*-2HG or solvent only (double-distilled H_2O, final concentration $\leq$ 3%) in the enzyme activity reaction medium. The 2HG:isocitrate and 2HG:αKG ratios used in these experiments are in line with the pathophysiological conditions in human glioma where *D*-2HG concentrations may be up to 100- to 1,000-fold higher than isocitrate and αKG concentrations (6).

Colony-forming assays after IR

Colony-forming assays after IR were performed and analyzed as described previously (33). Five to 500 cells/cm^2 were seeded; higher densities are needed at higher IR doses to obtain sufficient amounts of colonies. Cells were treated from 72 hours before to 4 hours after IR with *D*-2HG, AGI-5198, the reactive oxygen species (ROS) scavenger NAC, or solvent only (DMSO, $\leq$ 0.5%). Cells were irradiated with 1 to 6 Gy using a ^{137}Cs source (Department of Experimental Oncology and Radiobiology, Academic Medical Center, University of Amsterdam) at 6 hours after plating in the presence or absence of 0 to 800 nmol/L AGI-5198, 0 to 10 mmol/L *D*-2HG, or 0 to 5 μmol/L NAC. Cells were fixed and stained at 10 days after IR with a mixture of 0.05% crystal violet (Merck) and 6% glutaraldehyde (Merck) for $\geq$ 2 hours at room temperature. Clones consisting of $\geq$50 cells were manually counted using a stereoscope (Leica MZ6, Leica Microsystems; ref. 33). Data are expressed as clonogenic fraction,

Published OnlineFirst September 11, 2015; DOI: 10.1158/0008-5472.CAN-14-3603

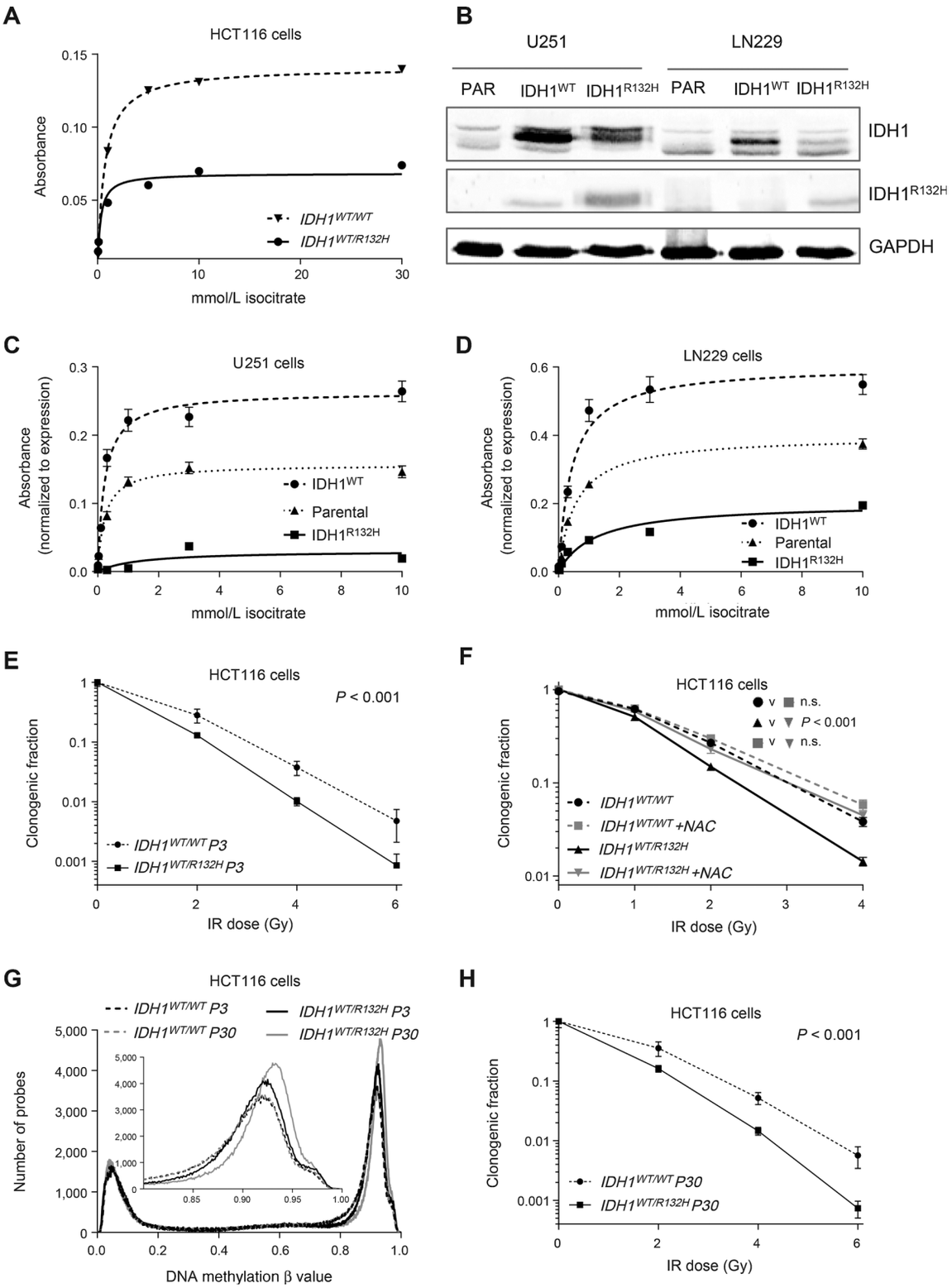

Figure 1.
IDH1^{R132H} mutations reduce IDH-mediated NADPH production and radioresistance. A, the $NADP^+$-dependent IDH activity of early-passage (P3) *IDH1*$^{WT/WT}$ and *IDH1*$^{WT/R132H}$ HCT116 cells at various isocitrate concentrations was determined as absorbance of blue formazan produced from NBT per cell. B, U251 and LN229 glioblastoma (parental) cell lines were stably transduced with lentiviral vectors harboring *IDH1*^{WT} and *IDH1*^{R132H} genes. All open reading frames have a C-terminal biotin acceptor peptide and a HIS tag for detection and purification purposes (not used in this work), which is why two IDH1 bands appear on the blot. The lower band is endogenous IDH1; the upper band is the tagged IDH1. Anti–pan-IDH1 antibody was used to detect IDH1^{WT} and IDH1^{R132H}. (*Continued on the following page.*)

Published OnlineFirst September 11, 2015; DOI: 10.1158/0008-5472.CAN-14-3603

which is the number of colonies counted divided by the number of cells plated, corrected for the plating efficiency. D_0 and n values were found by fitting a semilog line through the clonogenic fraction data points of the final slope. D_q values were found by solving the semilog line equation for 1.

Epigenome-wide DNA methylation analysis

Cells were lysed and genomic DNA was isolated as described previously (34). Genomic DNA was bisulfite-converted using the EZ DNA Methylation Gold Kit (Zymo Research). Bisulfite-converted DNA was analyzed for epigenome-wide DNA methylation analysis using an Infinium HumanMethylation 450 BeadChip array (Illumina). This array includes over 450,000 CpG sites that cover approximately 99% of the RefSeq genes. Analysis was performed in the MinFI R-package (R statistical programming language), and samples were normalized using the SWAN method (35). Normalized β-values were evaluated. Values are between 0 and 1, which stand for a completely unmethylated and methylated probe, respectively.

Cellular $NADP^+$, NADPH, GSH, GSSG, and ROS measurements

10^6 cells were plated in a 6-well plate, incubated in the presence or absence of 800 nmol/L AGI-5198, and treated with 0 to 2 Gy IR. After 60 minutes, cells were harvested, prepared, and analyzed for $NADP^+$/NADPH ratios, GSH/GSSG ratios, and ROS levels using a colorimetric $NADP^+$/NADPH Ratio Detection Assay Kit (Abcam), a fluorometric GSH/GSSG Ratio Detection Assay Kit (Abcam), and a fluorometric CellROX Deep Red ROS detection assay kit (Life Technologies), respectively, in a 96-well plate using a POLARStar Galaxy microplate reader (BMG Labtech) according to the manufacturers' protocols. In addition, cells were analyzed for ROS levels using a CellROX Deep Red ROS detection assay kit (Life Technologies) in an LSR Fortessa fluorescence flow cytometry analyzer (BD Biosciences) according to the manufacturer's protocol. Cells were counterstained using a SYTOX Blue Dead Cell Stain (Life Technologies). Data were processed in FACSDiva (BD Biosciences) and analyzed in FlowJo (FlowJo).

γ-H2AX immunofluorescence staining and measurements

DNA double-strand breaks (DSB) kinetics were studied using γ-H2AX foci immunofluorescence staining (36). Cells were plated on glass coverslips in a 6-well plate, incubated in the presence or absence of 800 nmol/L AGI-5198, and treated with 0 to 2 Gy IR, washed with PBS and fixed after 30 minutes using 2% paraformaldehyde for 15 minutes. Cells were permeabilized with pTNBS (PBS containing 1% Triton X-100 and 1% FCS) for 1 hour and stained for γ-H2AX foci using a mouse monoclonal anti–γ-H2AX antibody [Millipore; diluted 1:100 in sTNBS (PBS containing 0.1% Triton X-100 and 1% FCS)] for 90 min at room temperature. Cover slips were washed with sTNBS and stained using secondary goat anti-mouse Cy3 antibody (Jackson ImmunoResearch, diluted 1:100 in sTNBS) for 30 minutes at room temperature in the dark. Lastly, cover slips were washed with sTNBS, and nuclei were stained with DAPI (Millipore, 1:500) for 2 minutes at room temperature. Cover slips were mounted to microscopy slides using Vectashield (Vector Laboratories). Nail polish was used as sealant.

The number of γ-H2AX foci per cell was determined using a Leica DM RA HC fluorescence microscope equipped with a CCD camera and a 100× objective Plan Apochromatic lens with 1.40 numerical aperture (Leica Microsystems). Cy3 and DAPI signals were captured using excitation/emission wavelengths of 550/570 nm for 400 ms and 360/460 nm for 50 ms, respectively. Photomicrographs were obtained using custom-made software (Van Leeuwenhoek Center for Advanced Microscopy, Academic Medical Center, Amsterdam, the Netherlands). Stack images of at least 200 cells per sample were taken. One stack consisted of 40 slices with a 300-nm interval between the slices along the z-axis. The images were processed using deconvolution software, and the number of γ-H2AX foci per cell was automatically scored using custom-made software.

Statistical analysis

Data were processed in Excel (Microsoft) and analyzed using SPSS (IBM) and GraphPad Prism 6 (GraphPad Software). Nonlinear least squares were used to fit enzyme models. Data shown are representative of, or mean ± SEM of, at least three independent experiments. *P* values were calculated as described in the Materials and Methods section and figure legends; *, $P < 0.05$; **, $P < 0.01$; ***, $P < 0.001$; ****, $P < 0.0001$.

Results

IDH1*^{MT} reduce IDH-mediated NADPH production and IR tolerance *in vitro

$NADP^+$-dependent IDH activity was significantly lower in *lDH1*$^{WT/R132H}$ HCT116 cells than in *lDH1*$^{WT/WT}$ HCT116 cells (Fig. 1A; Supplementary Fig. S1A). The reduced IDH-mediated NADPH production capacity of *IDH1*^{MT} cells was confirmed in U251 and LN229 glioblastoma cell lines that stably overexpressed IDH1^{WT} or IDH1^{R132H} (Fig. 1B–D). Cells overexpressing IDH1^{WT} had a higher IDH-mediated NADPH production capacity than parental glioblastoma cells.

The vulnerability of *lDH1*$^{WT/R132H}$ and *lDH1*$^{WT/WT}$ HCT116 cells to IR was investigated using colony-forming assays. Relative to *IDH1*$^{WT/WT}$ cells, we observed a significantly reduced surviving fraction of *IDH1*$^{WT/R132H}$ cells at all IR doses (Fig. 1E), i.e., IDH1^{R132H} radiosensitizes HCT116 cells. We hypothesized that the increased radiosensitivity of *lDH1*$^{WT/R132H}$ HCT116 cells was caused by increased vulnerability to oxidative stress, which is a result of reduced IDH-mediated NADPH production capacity. To test this, we treated *lDH1*$^{WT/R132H}$ and *lDH1*$^{WT/WT}$ HCT116 cells with the NADPH surrogate and ROS scavenger NAC at 4 hours before IR.

(*Continued.*) A specific antibody against IDH1^{R132H} was used for detection of the IDH1^{R132H}-mutant enzyme. GAPDH served as a loading control. C and D, as in A, but with IDH1^{R132H}- and IDH1^{WT}-overexpressing glioblastoma cell lines U251 (C) and LN229 (D). To control for overexpression artifacts, enzyme activity of IDH1^{R132H}- and IDH1^{WT}-overexpressing cells was normalized relative to the enzyme activity of parental cells based on pan-IDH1 expression levels as determined by Western blot. E, colony-forming assay after 0 to 6 Gy IR with *IDH1*$^{WT/WT}$ and *IDH1*$^{WT/R132H}$ HCT116 cells. The clonogenic fraction is the number of colonies counted divided by the number of cells plated, corrected for the plating efficiency. F, as in E, but in the presence or absence of 5 μmol/L of ROS-scavenging NAC. G, β-values frequency plot of P3 and P30 *IDH1*$^{WT/WT}$ and *IDH1*$^{WT/R132H}$ HCT116 cells that were subjected to epigenome-wide DNA methylation analysis to determine whether *IDH1*^{R132H} induced a DNA hypermethylator phenotype after long-term culture. β-Values were between 0 and 1 and represent completely unmethylated and methylated probes, respectively. Inset, magnified plot of β-values between 0.8 and 1. H, as in E, but with P30 *IDH1*$^{WT/WT}$ and *IDH1*$^{WT/R132H}$ HCT116 cells. *Y*-axis in E, F, and H is logarithmic. v, versus; n.s., not significant.

Published OnlineFirst September 11, 2015; DOI: 10.1158/0008-5472.CAN-14-3603

NAC equalized the surviving fractions of *lDH1*$^{WT/R132H}$ and *IDH1*$^{WT/WT}$ HCT116 cells (Fig. 1F). This suggests that oxidative stress mediates the increased radiosensitivity of *lDH1*$^{WT/R132H}$ HCT116 cells. The culture medium McCoy 5A contains 0.5 mg/L reduced glutathione, which may affect redox potentials of HCT116 and therefore their IR response. We confirmed the increased radiosensitivity of *lDH1*$^{WT/R132H}$ HCT116 cells in DMEM medium, which contains no reduced glutathione (Supplementary Fig. S1B).

IDH^{MT} induce CIMP after long-term passaging of cells (9). CIMP has profound effects on gene expression and, theoretically, this could alter IR sensitivity. We compared genome-wide methylation levels in early-passage (P3) and late-passage (P30) *lDH1*$^{WT/R132H}$ and *lDH1*$^{WT/WT}$ HCT116 cells and observed a relative CIMP in P30 compared with P3 *lDH1*$^{WT/R132H}$ HCT116 cells. Long-term culture did not induce CIMP in *lDH1*$^{WT/WT}$ HCT116 cells (Fig. 1G). IR sensitivity of P30 *lDH1*$^{WT/R132H}$ HCT116 cells (Fig. 1H) did not differ from IR sensitivity of P3 *lDH1*$^{WT/R132H}$ HCT116 cells (Fig. 1E), and IR sensitivity is thus not related to CIMP. Statistics and D_q, n, and D_0 values for all colony-forming assays are shown in Supplementary Tables S1 and S2.

D-2HG sensitizes cells to IR and inhibits IDH-mediated NADPH production

A hallmark of *IDH*^{MT} cancer is *D*-2HG accumulation (1, 6), and *D*-2HG is known to induce oxidative stress in glia, neurons (37–39), and Drosophila (40). Therefore, we considered the possibility that *D*-2HG is responsible for the sensitization of *lDH1*$^{WT/R132H}$ HCT116 cells to IR. *lDH1*$^{WT/WT}$ and *lDH1*$^{WT/R132H}$ HCT116 cells were exposed to *D*-2HG from 4 hours before to 4 hours after IR treatment. *D*-2HG significantly decreased the clonogenic fractions of *lDH1*$^{WT/WT}$ and *lDH1*$^{WT/R132H}$ HCT116 cells after IR (Fig. 2A), i.e., *D*-2HG radiosensitizes HCT116 cells. Of note, the radiosensitizing effect of *D*-2HG was larger in *lDH1*$^{WT/WT}$ than in *lDH1*$^{WT/R132H}$ HCT116 cells, in line with pre-existing endogenous *D*-2HG in *lDH1*$^{WT/R132H}$ HCT116 cells.

D-2HG and *L*-2HG are competitive inhibitors of αKG-dependent enzymes (7, 8, 41). The structural similarity between isocitrate, αKG, and *D*-2HG led us to hypothesize that high levels of *D*-2HG in *IDH*^{MT} cancers inhibit IDH-mediated NADPH production capacity. To study this, we performed enzyme activity experiments in the presence and absence of *D*-2HG or *L*-2HG. *D*-2HG and *L*-2HG reduced the IDH-mediated NADPH production capacity in *lDH1*$^{WT/WT}$ and *lDH1*$^{WT/R132H}$ HCT116 cells, U251 glioblastoma cells, and *IDH1*^{WT} and *IDH1*^{MT} human glioblastoma tissue ($n = 8$; Fig. 2B–E); this inhibition was dose-dependent (Supplementary Fig. S2A). In addition, *D*-2HG and *L*-2HG inhibited the αKGDH-mediated NADH production capacity in *IDH1*^{WT} and *IDH1*^{MT} human glioblastoma tissue ($n = 8$; Fig. 2E and F). For both IDH and αKGDH, *L*-2HG was a more efficient IDH inhibitor than *D*-2HG. These results indicate that *D*-2HG and *L*-2HG are inhibitors of IDH-mediated NADPH production capacity. *D*-2HG and *L*-2HG did not affect G6PD-mediated NADPH production capacity or IDH-dependent NADH production capacity, indicating absence of off-target effects (Supplementary Fig. S2B and S2C).

The IDH1^{MT} inhibitor AGI-5198 restores IDH-mediated NADPH production in *IDH1*^{MT} cells

Since the introduction of IDH1^{R132H} increases metabolic stress via a reduced NADPH production capacity, we hypothesized that IDH1^{R132H} inhibition reverses this effect. Indeed, after 72 hours of incubation in the presence of AGI-5198, IDH-mediated NADPH production capacity of *lDH1*$^{WT/R132H}$ HCT116 cells was restored to levels comparable with those of *lDH1*$^{WT/WT}$ HCT116 cells (Fig. 3A). In contrast, no effect was detected after 4 hours of incubation with AGI-5198 (Fig. 3B) or in *lDH1*$^{WT/R132H}$ HCT116 cells that were treated with AGI-5198 after adherence to microscopical slides (Supplementary Fig. S3A). This suggests that AGI-5198 restores IDH-mediated NADPH production capacity after relieving *IDH1*$^{WT/R132H}$ cells of high *D*-2HG concentrations. We validated these results in IDH1^{R132H} U251 and LN229 cells (Fig. 3C and D). IDH1^{R132H} U251 cells needed the highest AGI-5198 doses for restoration of IDH-mediated NADPH production capacity, followed by IDH1^{R132H} LN229 cells, followed by *IDH1*$^{WT/R132H}$ HCT116 cells. This may relate to higher IDH1^{R132H} expression in U251 than in LN299 cells and higher IDH1^{R132H} expression in IDH1^{R132H}-overexpressing cells than in *IDH1*$^{WT/R132H}$ knock-in cells (Fig. 1B; Supplementary Fig. S1C). Larger amounts of IDH1^{R132H} protein may require higher AGI-5198 doses for complete IDH1^{R132H} inhibition. There was no effect after 72-hour incubation with AGI-5198 on $NADP^+$-dependent IDH activity in *lDH1*$^{WT/WT}$ HCT116 cells (Fig. 3E and F) or NAD^+-dependent IDH3 activity in *lDH1*$^{WT/R132H}$ HCT116 cells (Supplementary Fig. S3D), in agreement with AGI-5198 specificity for IDH1^{R132H} (23). Because AGI-5198 inhibits IDH1^{R132C} as well, although at higher concentrations than IDH1^{R132H} (23), we confirmed our results in *IDH1*$^{WT/R132C}$ HT1080 cells (Supplementary Fig. S3C and S3D).

IDH1^{MT} decrease NADPH and GSH levels and increase ROS levels and AGI-5198 attenuates this effect

We investigated the effects of *IDH1*^{MT} on cellular NADPH, GSH, and ROS levels with and without pretreatment with IR. Under steady-state conditions, *lDH1*$^{WT/R132H}$ HCT116 cells had similar $NADP^+$/NADPH ratios, GSH/GSSG ratios, and ROS levels as *lDH1*$^{WT/WT}$ HCT116 cells, as determined by colorimetric and fluorometric assays and fluorescence flow cytometry experiments (Fig. 4A–D; Supplementary Fig. S4). After treatment with 2 Gy IR, we observed an increase in the $NADP^+$/NADPH ratio (owing to more $NADP^+$ and/or less NADPH), a decrease in the GSH/GSSG ratio (owing to less GSH and/or more GSSG), and an increase in ROS levels in all cell lines. Notably, the increase in the $NADP^+$/NADPH ratio and ROS levels and the decrease in the GSH/GSSG ratio were larger in *lDH1*$^{WT/R132H}$ than in *lDH1*$^{WT/WT}$ HCT116 cells, and the IDH1^{MT} inhibitor AGI-5198 attenuated this effect in *lDH1*$^{WT/R132H}$ HCT116 cells (Fig. 4C and D). These findings suggest that compared with *lDH1*$^{WT/WT}$ HCT116 cells, the higher ROS levels in *lDH1*$^{WT/R132H}$ HCT116 cells after IR result in a higher GSH and NADPH consumption.

AGI-5198 protects *IDH1*^{MT} cells against IR

Because reduced NADPH production capacity in *lDH1*$^{WT/R132H}$ cells is associated with radiosensitization (Fig. 1), we hypothesized that by restoring NADPH production capacity in *lDH1*^{MT} cells, the lDH1^{MT} inhibitor AGI-5198 radioprotects *IDH1*^{MT} cells. Therefore, we exposed *lDH1*$^{WT/R132H}$ and *lDH1*$^{WT/WT}$ HCT116 cells to AGI-5198 for 72 hours before IR. AGI-5198 did not affect radiosensitivity of *lDH1*$^{WT/WT}$ HCT116 cells, but reduced radiosensitivity of *lDH1*$^{WT/R132H}$ HCT116 cells, in a dose-dependent fashion, to radiosensitivity levels comparable with those of *lDH1*$^{WT/WT}$ HCT116 cells (Fig. 5A and B). These data show that AGI-5198 radioprotects *lDH1*$^{WT/R132H}$ HCT116 cells and that high AGI-5198 doses completely block IDH1^{R132H}-induced

Published OnlineFirst September 11, 2015; DOI: 10.1158/0008-5472.CAN-14-3603

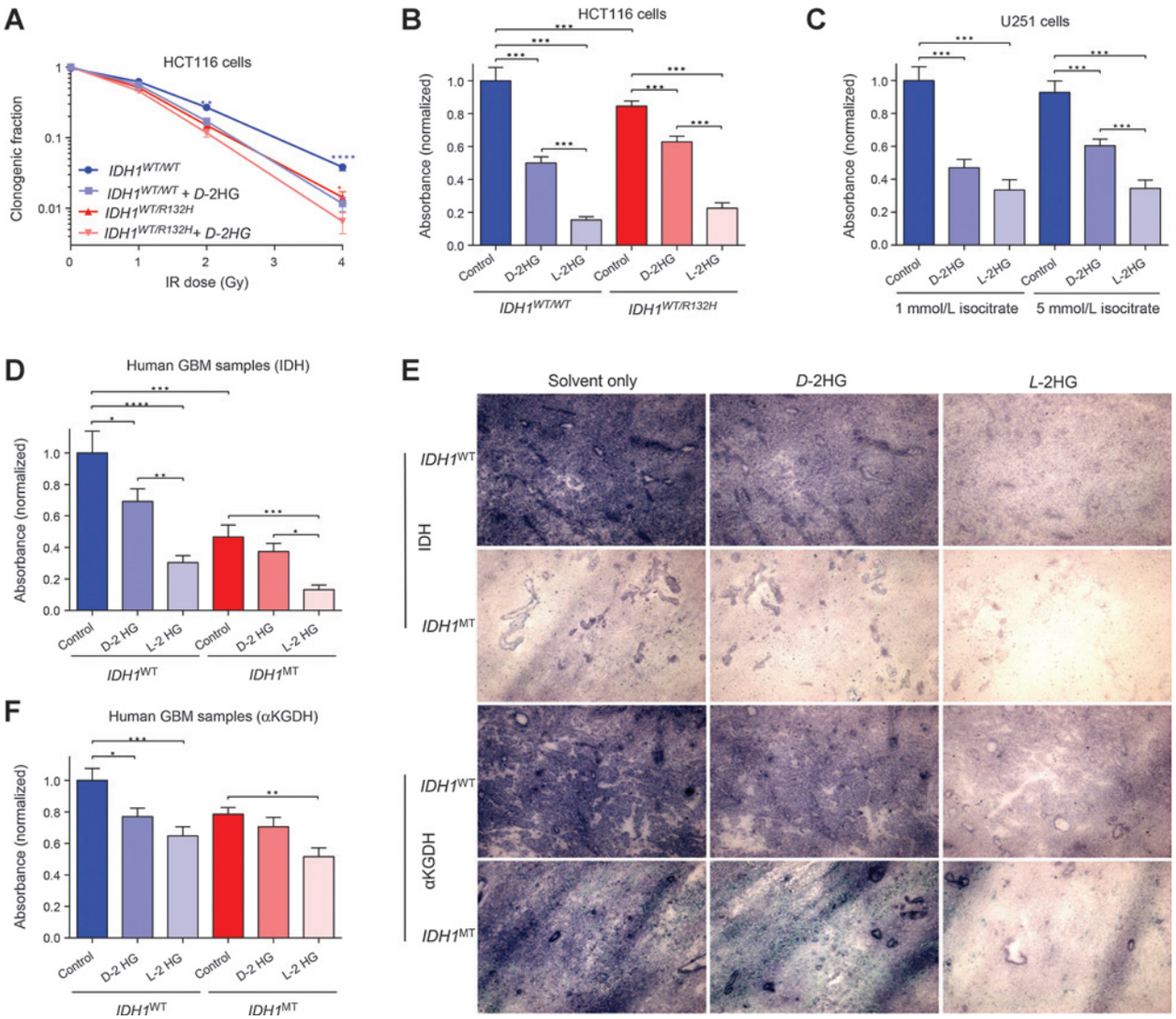

Figure 2.

D-2HG radiosensitizes cells and inhibits IDH-mediated NADPH production capacity. A, colony-forming assay after 0 to 4 Gy IR with *IDH1*$^{WT/WT}$ and *IDH1*$^{WT/R132H}$ HCT116 cells in the presence or absence of 10 mmol/L *D*-2HG. *D*-2HG incubation was from 4 hours before to 4 hours after IR. The clonogenic fraction is the number of colonies counted divided by the number of cells plated, corrected for the plating efficiency. *Y*-axis is logarithmic. B–D, the $NADP^+$-dependent IDH activity against 1 mmol/L isocitrate of *IDH1*$^{WT/WT}$ and *IDH1*$^{WT/R132H}$ HCT116 cells (B), U251 glioblastoma cells (C), and *IDH1* wild-type and *IDH1*-mutated human glioblastoma samples (D) was determined in the presence or absence of 30 mmol/L *D*-2HG or 30 mmol/L *L*-2HG. Absorbance of blue formazan produced from NBT was measured per cell (HCT116 and U251 cell lines) or per 0.5 mm × 0.5 mm tissue (human glioblastoma samples). In the latter case, serial sections were used. E, representative photomicrographs of serial sections of human glioblastoma samples after staining for $NADP^+$-dependent IDH activity and NAD^+-dependent αKGDH activity against 1 mmol/L isocitrate or 3 mmol/L αKG in the presence or absence of 30 mmol/L *D*-2HG or 30 mmol/L *L*-2HG. F, as in D, but with NAD^+-dependent αKGDH activity. *P* values were obtained using one-way ANOVA using Tukey correction for multiple comparisons. GBM, glioblastoma; *IDH1*^{WT}, *IDH1* wild-type; *IDH1*^{MT}, *IDH1*-mutated; αKGDH, α-ketoglutarate dehydrogenase.

radiosensitivity. We confirmed these findings in $IDH1^{R132H}$-overexpressing U251 glioblastoma cells (Fig. 5C), where higher AGI-5198 doses were needed to reach a maximal effect. This is in agreement with our finding that higher AGI-5198 doses were needed to restore the IDH-mediated NADPH production capacity in U251 cells than in *HCT116* cells (Fig 3A and C). No effect on radiosensitivity of *lDH1*$^{WT/R132H}$ HCT116 cells was observed after 4 hours of incubation with AGI-5198 (Fig. 5D). AGI-5198 was unable to radioprotect *lDH1*$^{WT/R132H}$ or *lDH1*$^{WT/WT}$ HCT116 cells in the presence of *D*-2HG (Fig. 5E), so the radioprotective mechanism of AGI-5198 on *lDH1*$^{WT/R132H}$ HCT116 cells depends predominantly on the inhibition of $IDH1^{R132H}$-mediated *D*-2HG production.

IDH1^{MT} increase numbers of DNA DSBs and AGI-5198 reverses this effect

DNA DSBs are important mediators of IR-induced cell death (36). We therefore hypothesized that $IDH1^{MT}$ cells are radiosensitized because they have increased numbers of DNA DSBs after IR. *lDH1*$^{WT/R132H}$ HCT116 cells had more γ-H2AX foci after treatment

Published OnlineFirst September 11, 2015; DOI: 10.1158/0008-5472.CAN-14-3603

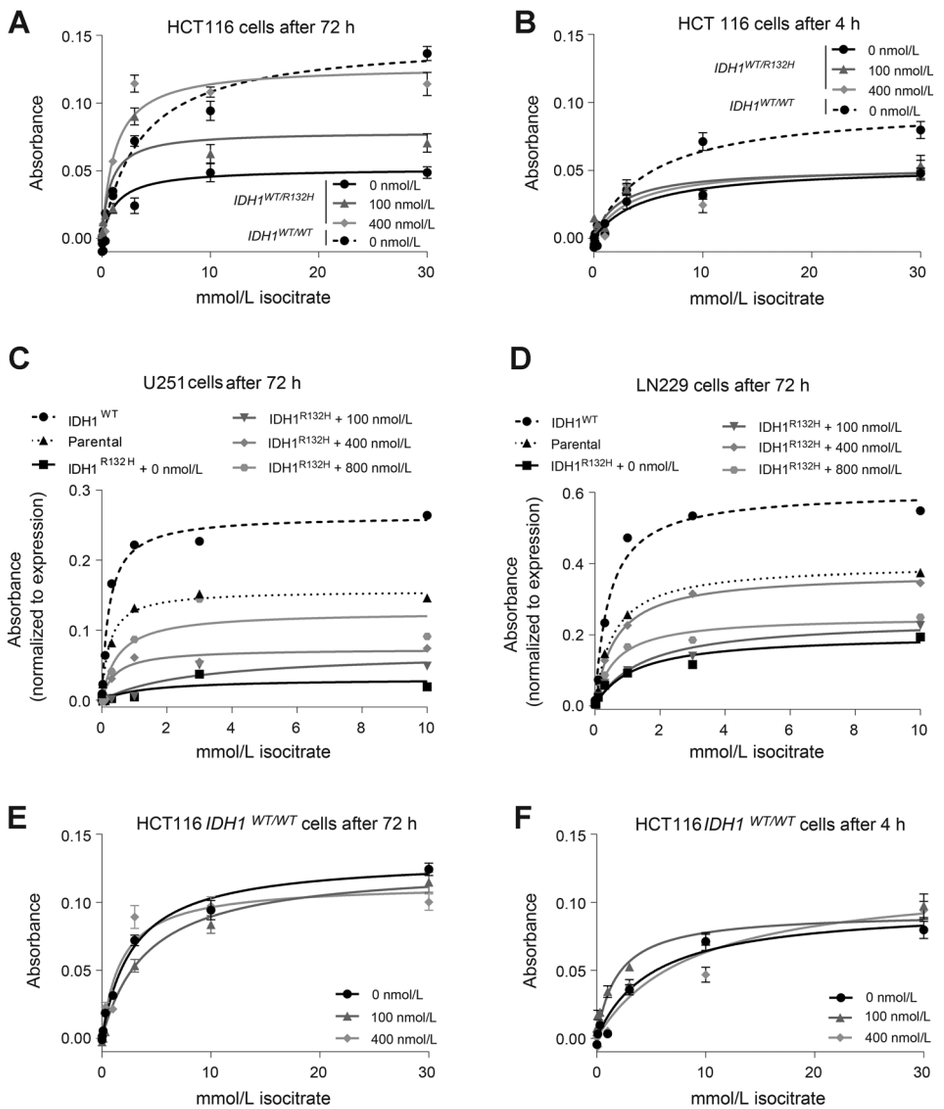

Figure 3.
The IDH1-mutant inhibitor AGI-5198 increases IDH-mediated NAPDH production capacity in *IDH1*-mutated cells. A, the $NADP^+$-dependent IDH activity of $IDH1^{WT/WT}$ and $IDH1^{WT/R132H}$ HCT116 cells at various isocitrate concentrations was determined as absorbance of blue formazan produced from NBT per cell after 72-hour cell culture in the presence or absence of AGI-5198. B, as in A, but after 4-hour cell culture in the presence or absence of AGI-5198 instead of 72 hours. C, as in A, but using parental, $IDH1^{WT}$-overexpressing, and $IDH1^{R132H}$-overexpressing U251 cells. D, as in C, but using LN229 cells. E and F, as in A and B, but using $IDH1^{WT/WT}$ HCT116 cells only. All concentrations in the figure refer to AGI-5198.

with 1 or 2 Gy of IR than $lDH1^{WT/WT}$ HCT116 cells, and AGI-5198 decreased the numbers of γ-H2AX foci after IR in $lDH1^{WT/R132H}$, but not in $lDH1^{WT/WT}$ HCT116 cells (Fig. 6A and B).

IDH1^{MT} increase sensitivity to metformin and AGI-5198 protects *IDH1*^{MT} cells against metformin

We wondered whether the increased sensitivity of $lDH1^{WT/R132H}$ HCT116 cells was specific to IR or also applicable to other treatment modalities that induce stress. $IDH1^{MT}$ cells are sensitized to antidiabetic biguanides such as metformin (42, 43), which also depend on oxidative stress to induce cell death (44). We treated $lDH1^{WT/R132H}$ and $lDH1^{WT/WT}$ HCT116 cells with 0 to 6 mmol/L metformin in a proliferation experiment. Relative to untreated cells, we observed less $lDH1^{WT/R132H}$ than $lDH1^{WT/WT}$ HCT116 cells after metformin treatment (Supplementary Fig. S5). Moreover, $lDH1^{WT/R132H}$ HCT116 cells that were treated with both AGI-5198 and metformin proliferated more than $lDH1^{WT/R132H}$ HCT116 cells treated with metformin alone. This indicates that $lDH1^{WT/R132H}$ HCT116 cells are sensitized to stress induced by IR or metformin and that AGI-5198 protects $lDH1^{WT/R132H}$ HCT116 cells against both treatment modalities.

Discussion

We showed that introduction of $IDH1^{R132H}$ results in *D*-2HG accumulation, inhibits IDH^{WT} function, and sensitizes cells to IR and metformin. The overall process can thus be described as a *D*-2HG-NADPH-therapy sensitivity cascade for $IDH1^{MT}$ cancer cells (Fig. 7). Inhibition of $IDH1^{MT}$ by AGI-5198 disrupts this cascade at the level of *D*-2HG production, which enhances the capacity of $IDH1^{MT}$ cells to reduce oxidative stress and protects them against IR and metformin.

Patients with glioma or cholangiocarcinoma tumors carrying IDH^{MT} have prolonged overall survival compared with IDH^{WT} counterparts (3, 5, 10, 11). This can be attributed to intrinsic (e.g., less aggressive tumors) and/or extrinsic (e.g., better response to therapy) differences in IDH^{MT} versus IDH^{WT} cancers. Our data support a correlation between IDH^{MT} and response to therapy,

Published OnlineFirst September 11, 2015; DOI: 10.1158/0008-5472.CAN-14-3603

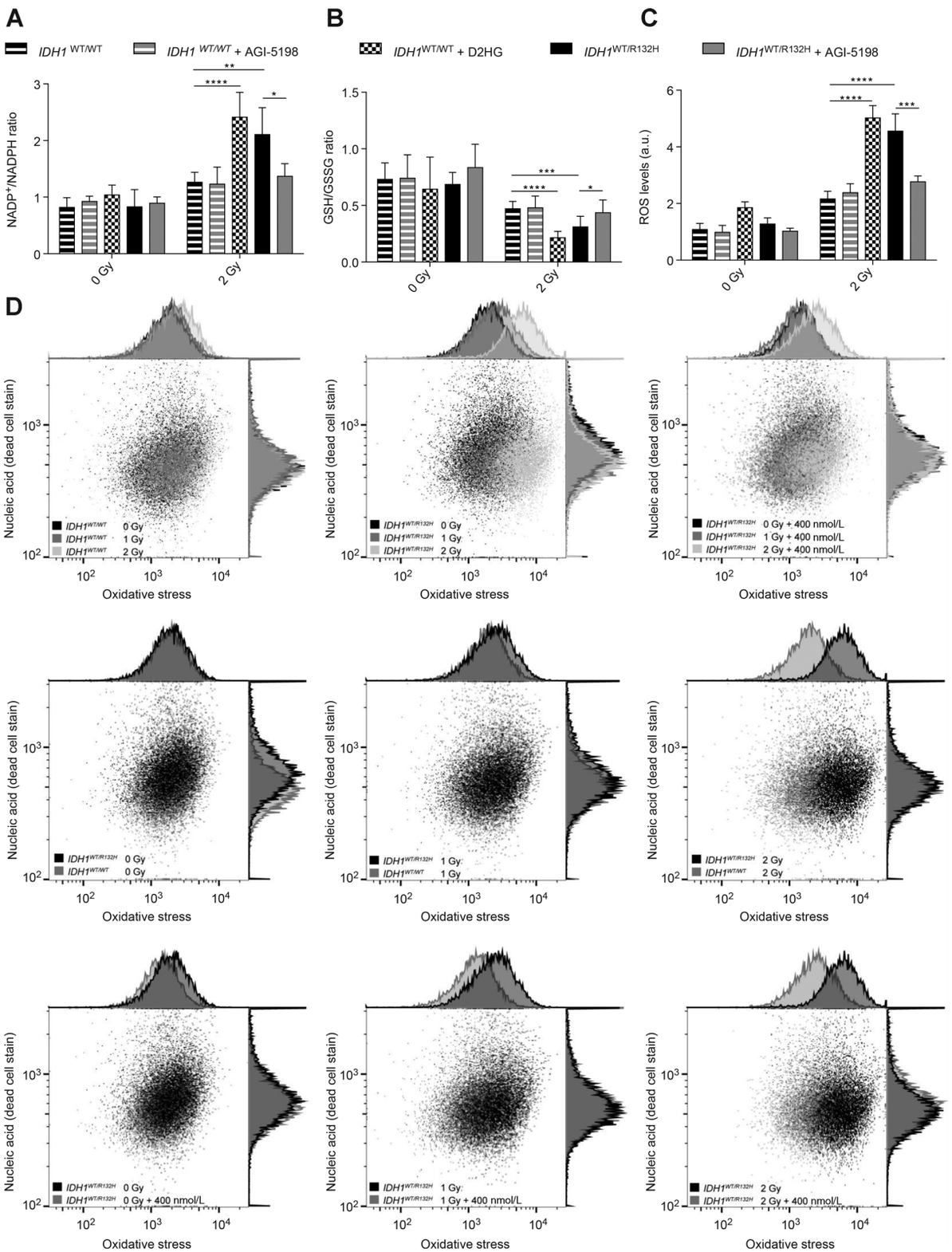

Figure 4.
IDH1^{MT} decrease NADPH levels and GSH levels, increase ROS levels, and AGI-5198 attenuates this effect. A, cells were incubated in the presence or absence of 800 nmol/L AGI-5198 and treated with 0 to 2 Gy IR and were harvested, prepared, and colorimetrically analyzed for $NADP^+$/NADPH ratios after 60 minutes. B, as in A, but with fluorometric analysis for GSH/GSSG ratios. C, as in A, but with fluorometric analysis for ROS levels. D, as in C, but with fluorescence-guided flow cytometry analysis for ROS levels (*x*-axis) and viable cells (*y*-axis). *P* values were obtained using one-way ANOVA on the difference between IR-treated and untreated cells using Tukey correction for multiple comparisons. All concentrations in the figure refer to AGI-5198.

Published OnlineFirst September 11, 2015; DOI: 10.1158/0008-5472.CAN-14-3603

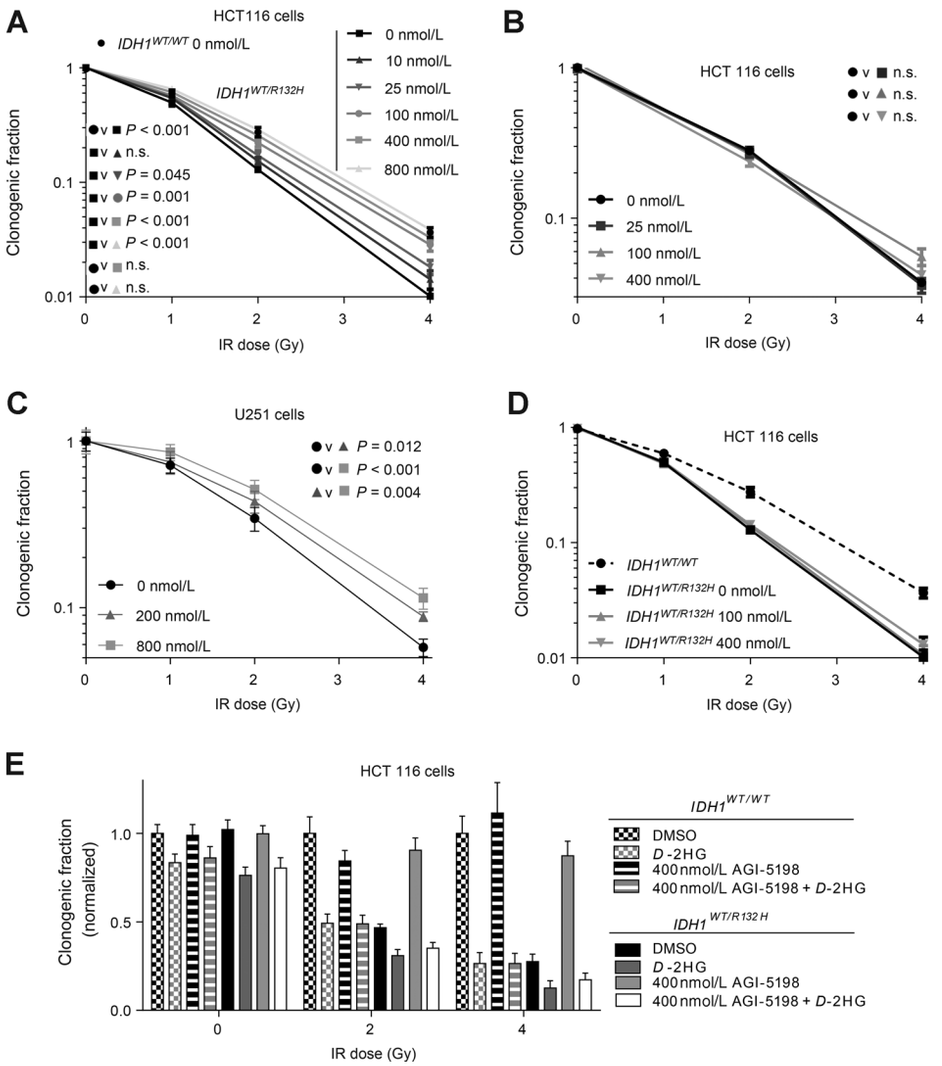

Figure 5.
IDH1-mutant inhibitor AGI-5198 dose-dependently radioprotects *IDH1*-mutated cells. A, colony-forming assay after 0 to 4 Gy IR with $IDH1^{WT/WT}$ and $IDH1^{WT/R132H}$ HCT116 cells after long-term (72 hours) incubation in the presence or absence of 0 to 400 nmol/L AGI-5198. The normalized clonogenic fraction is the number of colonies counted divided by the number of cells plated, corrected for the plating efficiency, and normalized to the clonogenic fraction of untreated, irradiated $IDH1^{WT/WT}$ HCT116 cells. B, colony-forming assay after 0 to 4 Gy IR with $IDH1^{WT/WT}$ HCT116 cells after long-term (72 hours) incubation in the presence or absence of 0 to 400 nmol/L AGI-5198. C, colony-forming assay after 0 to 4 Gy IR with $IDH1^{R132H}$-overexpressing U251 cells after long-term (72 hours) incubation in the presence or absence of 800 nmol/L AGI-5198. D, colony-forming assay after 0 to 4 Gy IR with $IDH1^{WT/WT}$ and $IDH1^{WT/R132H}$ HCT116 cells after short-term (4 hours) incubation in the presence or absence of 0 to 400 nmol/L AGI-5198. E, colony-forming assay after 0 to 4 Gy IR with $IDH1^{WT/WT}$ and $IDH1^{WT/R132H}$ HCT116 cells after long-term (72 hours) incubation in the presence or absence of 0 to 400 nmol/L AGI-5198 and/or 4-hour incubation in the presence or absence of 10 mmol/L *D*-2HG. *Y*-axis in B to D is logarithmic. All concentrations in the figure refer to AGI-5198. v, versus; n.s., not significant.

which has been shown by others, both *in vitro* (15–17) and retrospectively in the clinic (18, 19). Our novel finding is that *D*-2HG accumulation, as occurs in $IDH1^{MT}$ cancers, directly radiosensitizes cancer cells via inhibition of IDH-mediated NADPH production capacity and that this is associated with increased numbers of DNA DSBs after IR. Thus, the prolonged survival effects of IDH^{MT} in glioma patients may, at least partly, be the result of a relative radiosensitivity of $IDH1^{MT}$ cancer cells.

IDH^{MT} confer a worse prognosis in AML patients (45). One difference between AML and glioma is that IR is typically not used to treat AML, whereas it is routinely used as a treatment modality for glioma. Cytarabine and daunorubicin are used to treat AML and operate by DNA synthesis chain termination and topoisomerase activity, which cause cell death independent of ROS formation. Furthermore, *D*-2HG accumulation in AML cells has likely less biologic impact since NADPH production in leukocytes is largely attributable to activity of G6PD, not IDH1/2 (46). In contrast, IDH1/2 is responsible for 65% of NADPH production in glioblastoma, and $IDH1^{MT}$ decrease NADPH production capacity by 38% (5), making these tumors dependent on IDH1/2 for reducing power.

In addition to glioblastoma and chondrosarcoma cell lines, we used HCT116 colorectal carcinoma cells as *in vitro* model. Although $IDH1^{MT}$ are not as prevalent in colorectal carcinoma as in glioma, chondrosarcoma, or cholangiocarcinoma, they do occur in 0.5% of patients (47). Thus, $IDH1^{MT}$ may affect colorectal cancer cells similarly to glioma, cholangiocarcinoma, and chondrosarcoma cells. Because $IDH1^{R132H}$ functions as a heterodimer with $IDH1^{WT}$, 1:1 $IDH1^{R132H}$:$IDH1^{WT}$ expression in $IDH1^{WT/R132H}$ HCT116 cells is more true to nature than $IDH1^{R132H}$ overexpression. Previous reports (3, 5) have shown that the loss-of-function effects of $IDH1^{MT}$ are responsible for reduced IDH-mediated NADPH production capacity in $IDH1^{MT}$ tumors. In cancer cells, $IDH1^{R132H}$ mutations are heterozygous, i.e., cells lose one functional NADPH-producing allele. In addition, the net NADPH production in $IDH1^{MT}$ cells is further reduced via NADPH consumption by $IDH1^{R132H}$ (6). However, reductive hydroxylation of αKG by $IDH1^{R132H}$ occurs 100 to 1,000 times slower than the oxidative decarboxylation by IDH^{WT} (6, 48), so such compounding is likely negligible. The present study shows that $IDH1^{MT}$ reduce NADPH production capacity through a third mechanism: $IDH1^{R132H}$-produced *D*-2HG inhibits IDH^{WT}. This supports earlier

Published OnlineFirst September 11, 2015; DOI: 10.1158/0008-5472.CAN-14-3603

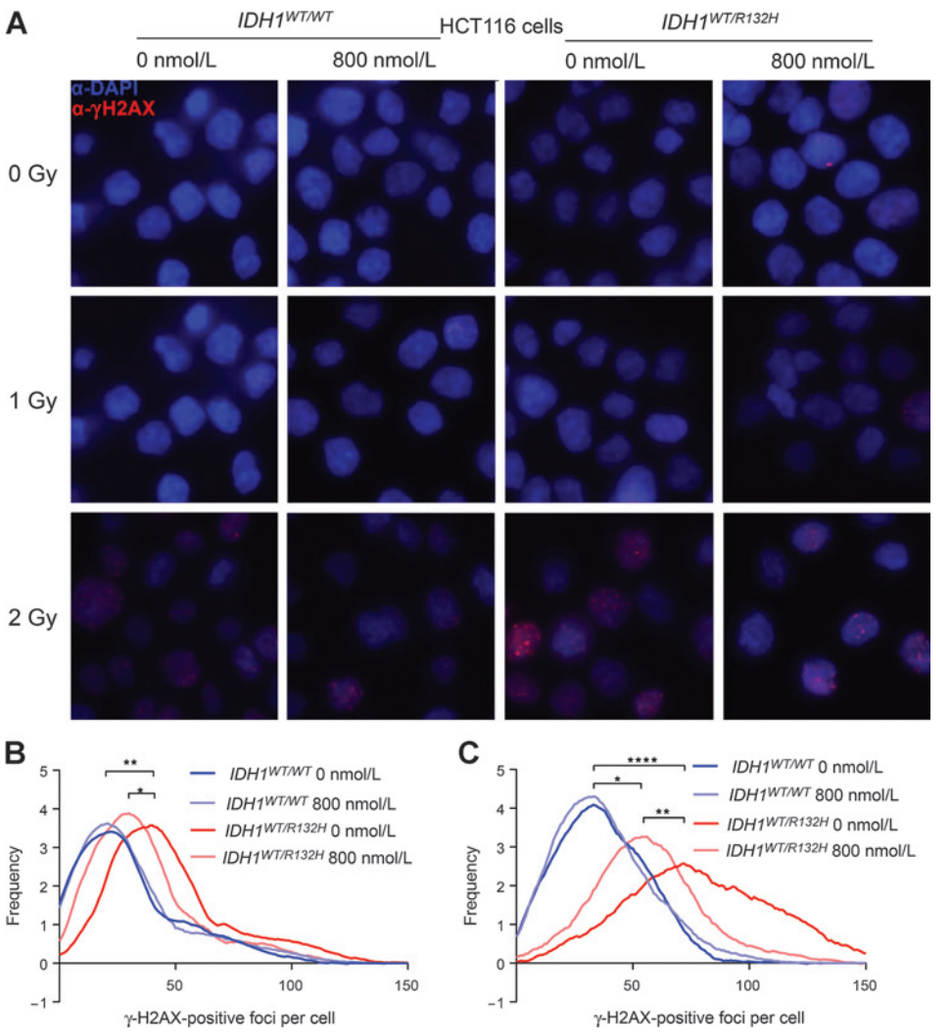

Figure 6.
IDH1^{MT} increase numbers of DNA DSBs and AGI-5198 reverses this effect. A, representative photomicrographs of cells that were plated on glass coverslips in the presence or absence of AGI-5198, treated with 0 to 2 Gy IR, and fixed after 30 minutes. Cells were stained immunocytochemically for γ-H2AX for DNA DSBs and with DAPI for DNA content. B and C, stack images (40 slices, 300 nm intervals) of at least 200 cells per sample were taken using a fluorescence microscope using custom-made software. Images were processed using deconvolution software, and the number of γ-H2AX–positive foci per cell was automatically scored using custom-made software. Sixth-order smoothing (25 neighbors) was applied to the curves. B, frequency plot of γ-H2AX–positive foci per cell for cells treated with 1 Gy IR. C, as in B, but with 2 Gy IR. All concentrations in the figure refer to AGI-5198. *P* values were obtained using one-way ANOVA on the difference between treated and untreated cells using Tukey correction for multiple comparisons.

findings that *IDH1*^{MT} inhibit catalytic IDH1^{WT} function in a dominant-negative fashion (4). We show that this dominant-negative inhibition is mediated by *D*-2HG. Another, but not mutually exclusive, explanation is that this dominant-negative inhibition is mediated by dysfunctional IDH1^{WT}-IDH1^{R132H} heterodimers (49). In addition to IDH^{WT}, *D*-2HG inhibits αKGDH and cytochrome *C* oxidase (complex IV of the electron transport chain; ref. 50), which further compromises tricarboxylic acid cycle metabolism in *IDH*^{MT} cells. AGI-5198 did not protect *lDH1*$^{WT/R132H}$ HCT116 cells against IR when exogenous *D*-2HG was administered. This supports the notion that NADPH consumption by IDH1^{R132H} does not radiosensitize *lDH1*$^{WT/R132H}$ HCT116 cells. Of note, *L*-2HG was a more potent inhibitor than *D*-2HG of IDH and αKGDH. This corroborates studies that showed that *L*-2HG is a more potent inhibitor than *D*-2HG of αKG-dependent enzymes, such as TET2, JHKDMs, and EGLN (7, 8).

AGI-5198 restored IDH-mediated NADPH production capacity and radioresistance of *IDH1*^{MT} cells, and both effects are likely the result of AGI-5198-inhibited *D*-2HG synthesis. High-dose AGI-5198 completely abolishes *D*-2HG accumulation (23) and completely rescued the radiosensitivity of *lDH1*$^{WT/R132H}$ HCT116 cells. Oxidative stress is a likely mediator of *IDH1*$^{WT/R132H}$ radiosensitization in HCT116 cells, because the ROS scavenger NAC normalized the radiosensitivity of *IDH1*$^{WT/R132H}$ HCT116 cells to levels of *IDH1*$^{WT/WT}$ HCT116 cells. In addition, *IDH1*^{MT} cells were also sensitized for treatment with metformin, whereas AGI-5198 protected *IDH1*^{MT} cells against metformin. This is in agreement with the fact that mitochondrial inhibitors such as metformin depend on oxidative stress to induce cell death (44). Previous reports have shown that *D*-2HG induces cellular oxidative stress (37–40), although the underlying mechanisms remained elusive thus far. Our data indicate that inhibition of IDH-mediated NADPH production capacity and αKGDH-mediated NADH production capacity by *D*-2HG and the resulting metabolic stress is, at least partly, responsible for this phenomenon. Our findings that *D*-2HG and *L*-2HG inhibit the activity of IDH^{WT} and αKGDH suggest that this inhibition is due to the chemical similarities between *D*-2HG, *L*-2HG, and αKG.

Long-lasting exposures of AGI-5198 (72 hours) radioprotected *IDH1*^{MT} cells but short exposures (4 hours) did not. These data corroborate our quantitative enzyme histochemistry results where 72-hour exposure to high doses of AGI-5198 completely restored IDH-mediated NADPH production capacity of *lDH1*^{MT} cells, but 4-hour exposures did not. This indicates that there is a delaying

Published OnlineFirst September 11, 2015; DOI: 10.1158/0008-5472.CAN-14-3603

A

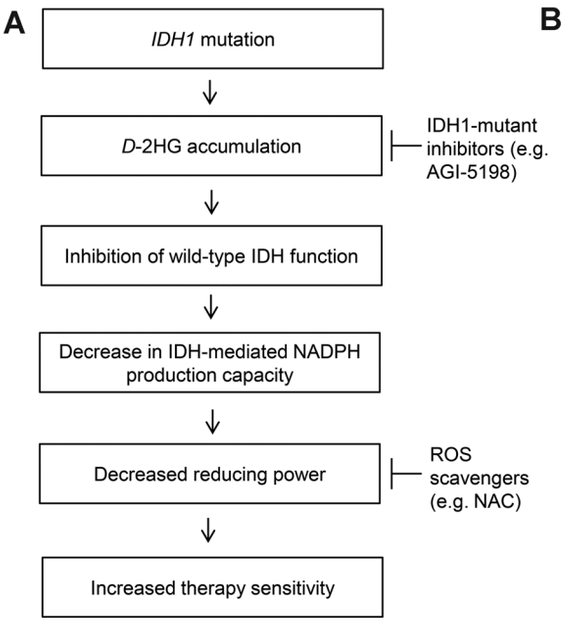

B

	D-2HG production	IDH activity	ROS generation	IR tolerance
IDH1^{R132H} mutation	↑ (6)	↓ [1A-D]	↑ [3C,D]	↓ [1E]
***D*-2HG administration**	N.D.	↓ [2B-E]	↑ [3C]	↓ [2A]
AGI-5198 exposure (72 h)	↓ (23,25)	↑ [3A,C]	↓ [3C,D]	↑ [5A,C,E]
AGI-5198 exposure (4 h)	= (25)	= [3B,D]	N.D.	= [5D]

Figure 7.
IDH1 mutations sensitize cancer cells against IR via a *D*-2HG-NADPH-radiosensitivity cascade. A, *D*-2HG-NADPH-radiosensitivity cascade for *IDH1*-mutated cancer cells. IDH1-mutant inhibitors such as AGI-5198 inhibit the production of *D*-2HG and thereby the ensuing steps in this cascade, ultimately resulting in an increased radioresistance of *IDH1*-mutated cancer cells. B, summary of findings. Corresponding figure numbers are between [] and corresponding references between (). ↑, increase; ↓, decrease; =, no effect; N.D., not determined.

intermediate that causes lagged AGI-5198–induced restoration of IDH-mediated NADPH production capacity and radioresistance. Our findings suggest that *D*-2HG is this intermediate and that *D*-2HG is metabolized slowly. This supports speculations that the activity of *D*-2HG dehydrogenase (*D*-2HGDH) is low (51). In addition, it is accordant with the finding that ML309, an IDH1^{MT} inhibitor similar to AGI-5198, maximally suppresses *D*-2HG concentrations when applied for at least 24 hours (25).

IDH1^{MT} decreased NADPH and GSH levels and increased ROS levels, but only when cells were treated with IR. This corroborates earlier studies in which *IDH1*^{MT} decreased NADPH and GSH levels and increased ROS in glioblastoma cells after treatment with temozolomide and CDDP (15), but not in a transgenic mouse model or glioblastoma cells under steady-state conditions (15, 52). Taken together, our results suggest that in contexts of stress, such as after treatment with IR, the cellular demand for GSH increases. As a consequence, the demand for NADPH increases, but *IDH1*^{MT} compromise the cellular NADPH production capacity, and this restricts recycling of GSSG to GSH enough to cause higher ROS levels, i.e., it causes a scenario in which NADPH demand outweighs NADPH supply. In all, our results suggest that altered oxidative stress response is the most likely downstream element of *D*-2HG that results in *IDH*^{MT} radiosensitivity. Oxidative stress can either directly induce cell death after treatment with IR, or indirectly via DNA DSBs. On average, *IDH1*$^{WT/R132H}$ HCT116 cells had twice the amount of DNA DSBs of *IDH1*$^{WT/WT}$ HCT116 cells after treatment with 2 Gy IR, but the amount of DNA DSBs was only slightly increased in *IDH1*$^{WT/R132H}$ compared with *IDH1*$^{WT/WT}$ HCT116 cells after treatment with 1 Gy IR. This resonates with a larger radiosensitivity of *IDH1*^{MT} cells relative to *IDH1*^{WT} cells after treatment with $\geq$ 2 Gy IR than after treatment with 1 Gy IR. Further research is needed to assess whether this is due to increased generation of DSBs by oxidative stress, or decreased DNA DSB repair, and whether *IDH*^{MT} cancers are sensitized to anticancer therapy that targets DNA DSB repair, such as PARP inhibitors. CIMP did not affect the radiosensitivity of *IDH*^{MT} cells, which argues against a role for epigenetics in this phenomenon. Moreover, long-term AGI-5198 treatment does not reverse CIMP in *IDH*^{MT} glioma cells (23), and this further precludes a link between CIMP and *IDH*^{MT} radiosensitivity, because AGI-5198 reverses *IDH*^{MT} radiosensitization already after 72 hours.

Clinical trials with IDH^{MT} inhibitors have already started in patients with *IDH*^{MT} cancer. Our data show that AGI-5198 antagonizes the possibly survival-prolonging radiosensitizing effects of *IDH1*^{MT} in glioma. Our *in vitro* results suggest that concomitant administration of IDH^{MT} inhibitors and IR may result in an unfavorable clinical outcome. *In vivo* validation is urgently necessary as IDH^{MT} inhibitors are already in clinical trials. These limitations may also apply to other therapeutic strategies that include a combination of IDH^{MT} inhibition with anticancer agents whose activity is mediated by oxidative stress. More specifically, we warn against simultaneous treatment with IDH^{MT} inhibitors and IR. Instead, we envision treatments in which conventional treatment modalities are applied subsequently, but not concomitantly, with IDH^{MT} inhibitors. IDH^{MT} inhibitors may be of clinical use when patients are in periods of recovery from conventional anticancer drugs whose activity is mediated by oxidative stress. We propose that personalized medicine for *IDH1*^{MT} solid tumors should aim to increase, not decrease, oxidative stress. This may be achieved by antitumor immune responses after immunization of patients with an IDH1^{R132H} peptide (53), causing inflammatory ROS, or physical exercise,

causing mitochondrial ROS (54). In addition, other Achilles' heels in *IDH*^{MT} metabolism could be exploited, such as mitochondrial dysfunction (50), increased dependence on glutaminolysis (2, 55–59) and oxidative phosphorylation (42, 43). These vulnerabilities can be pharmacologically targeted via BCL-2 inhibitors, chloroquine, and metformin, respectively.

In summary, our data show that AGI-5198 radioprotects IDH1^{MT} cancer cells. Administration of IDH^{MT} inhibitors during IR may thus abolish the prolonged survival of *IDH*^{MT} glioma patients. We warn against multiagent clinical trials with concomitant use of IDH^{MT} inhibitors and IR.

Disclosure of Potential Conflicts of Interest

J.P. Maciejewski has received speakers bureau honoraria from Alexion, Celgene, and Ra Pharma, and is a consultant/advisory board member for Alexion PNH Advisory Board. No potential conflicts of interest were disclosed by the other authors.

Authors' Contributions

Conception and design: R.J. Molenaar, D. Botman, C.M. van Drunen, T. Radivoyevitch, J.P. Maciejewski, W.P. Leenders, F.E. Bleeker, C.J. van Noorden
Development of methodology: R.J. Molenaar, D. Botman, J. Stap, M. Khurshed, W.P. Leenders, F.E. Bleeker
Acquisition of data (provided animals, acquired and managed patients, provided facilities, etc.): R.J. Molenaar, D. Botman, M.A. Smits, V.V. Hira, S. A. van Lith, K. Lenting, W.P. Vandertop
Analysis and interpretation of data (e.g., statistical analysis, biostatistics, computational analysis): R.J. Molenaar, D. Botman, M.A. Smits, V.V. Hira, J. Stap, P. Henneman, M. Khurshed, A.N. Mul, C.M. van Drunen, R.A. Hoebe, W.P. Leenders
Writing, review, and/or revision of the manuscript: R.J. Molenaar, D. Botman, S.A. van Lith, J. Stap, P. Henneman, M. Khurshed, K. Lenting, C.M. van Drunen, T. Radivoyevitch, J.W. Wilmink, J.P. Maciejewski, W.P. Vandertop, W.P. Leenders, F.E. Bleeker, C.J. van Noorden
Administrative, technical, or material support (i.e., reporting or organizing data, constructing databases): D. Botman, P. Henneman
Study supervision: R.J. Molenaar, J.P. Maciejewski, F.E. Bleeker, C.J. van Noorden
Other (conducted some experiments as an intern student): D. Dimitrakopoulou

Acknowledgments

The authors thank Wikky Tigchelaar-Gutter, Renske Hulsbos, Ece Nokay, Berend Hooibrink, Dr. Klaas Franken, Dr. Wiljan Hendriks, Ing. Jan Schepens, and Dr. Ard Jonker for technical support.

Grant Support

The research described in this report was supported by the Dutch Cancer Society (KWF; UVA 2014-6839). R.J. Molenaar was supported by an AMC PhD Scholarship.

The costs of publication of this article were defrayed in part by the payment of page charges. This article must therefore be hereby marked *advertisement* in accordance with 18 U.S.C. Section 1734 solely to indicate this fact.

Received December 9, 2014; revised August 6, 2015; accepted August 12, 2015; published OnlineFirst September 11, 2015.

References

1. Molenaar RJ, Radivoyevitch T, Maciejewski JP, van Noorden CJ, Bleeker FE. The driver and passenger effects of isocitrate dehydrogenase 1 and 2 mutations in oncogenesis and survival prolongation. Biochim Biophys Acta 2014;1846:326–41.
2. van Lith SA, Navis AC, Verrijp K, Niclou SP, Bjerkvig R, Wesseling P, et al. Glutamate as chemotactic fuel for diffuse glioma cells: are they glutamate suckers? Biochim Biophys Acta 2014;1846:66–74.
3. Yan H, Parsons DW, Jin G, McLendon R, Rasheed BA, Yuan W, et al. IDH1 and IDH2 mutations in gliomas. N Engl J Med 2009;360:765–73.
4. Zhao S, Lin Y, Xu W, Jiang W, Zha Z, Wang P, et al. Glioma-derived mutations in IDH1 dominantly inhibit IDH1 catalytic activity and induce HIF-1alpha. Science 2009;324:261–5.
5. Bleeker FE, Atai NA, Lamba S, Jonker A, Rijkeboer D, Bosch KS, et al. The prognostic IDH1(R132) mutation is associated with reduced NADP+-dependent IDH activity in glioblastoma. Acta Neuropathol 2010;119:487–94.
6. Dang L, White DW, Gross S, Bennett BD, Bittinger MA, Driggers EM, et al. Cancer-associated IDH1 mutations produce 2-hydroxyglutarate. Nature 2009;462:739–44.
7. Chowdhury R, Yeoh KK, Tian YM, Hillringhaus L, Bagg EA, Rose NR, et al. The oncometabolite 2-hydroxyglutarate inhibits histone lysine demethylases. EMBO Rep 2011;12:463–9.
8. Xu W, Yang H, Liu Y, Yang Y, Wang P, Kim SH, et al. Oncometabolite 2-hydroxyglutarate is a competitive inhibitor of alpha-ketoglutarate-dependent dioxygenases. Cancer Cell 2011;19:17–30.
9. Turcan S, Rohle D, Goenka A, Walsh LA, Fang F, Yilmaz E, et al. IDH1 mutation is sufficient to establish the glioma hypermethylator phenotype. Nature 2012;483:479–83.
10. Parsons DW, Jones S, Zhang X, Lin JC, Leary RJ, Angenendt P, et al. An integrated genomic analysis of human glioblastoma multiforme. Science 2008;321:1807–12.
11. Molenaar RJ, Verbaan D, Lamba S, Zanon C, Jeuken JW, Boots-Sprenger SH, et al. The combination of IDH1 mutations and MGMT methylation status predicts survival in glioblastoma better than either IDH1 or MGMT alone. Neuro Oncol 2014;16:1263–73.
12. Wang P, Dong Q, Zhang C, Kuan PF, Liu Y, Jeck WR, et al. Mutations in isocitrate dehydrogenase 1 and 2 occur frequently in intrahepatic cholangiocarcinomas and share hypermethylation targets with glioblastomas. Oncogene 2013;32:3091–100.
13. Labussiere M, Sanson M, Idbaih A, Delattre JY. IDH1 gene mutations: a new paradigm in glioma prognosis and therapy? Oncologist 2010;15:196–9.
14. Abdel-Wahab O, Levine RL. Metabolism and the leukemic stem cell. J Exp Med 2010;207:677–80.
15. Shi J, Sun B, Shi W, Zuo H, Cui D, Ni L, et al. Decreasing GSH and increasing ROS in chemosensitivity gliomas with IDH1 mutation. Tumour Biol 2015;36:655–62.
16. Mohrenz IV, Antonietti P, Pusch S, Capper D, Balss J, Voigt S, et al. Isocitrate dehydrogenase 1 mutant R132H sensitizes glioma cells to BCNU-induced oxidative stress and cell death. Apoptosis 2013;18:1416–25.
17. Li S, Chou AP, Chen W, Chen R, Deng Y, Phillips HS, et al. Overexpression of isocitrate dehydrogenase mutant proteins renders glioma cells more sensitive to radiation. Neuro Oncol 2013;15:57–68.
18. Cairncross JG, Wang M, Jenkins RB, Shaw EG, Giannini C, Brachman DG, et al. Benefit from procarbazine, lomustine, and vincristine in oligodendroglial tumors is associated with mutation of IDH. J Clin Oncol 2014;32:783–90.
19. Tran AN, Lai A, Li S, Pope WB, Teixeira S, Harris RJ, et al. Increased sensitivity to radiochemotherapy in IDH1 mutant glioblastoma as demonstrated by serial quantitative MR volumetry. Neuro Oncol 2014;16:414–20.
20. Bleeker FE, Molenaar RJ, Leenstra S. Recent advances in the molecular understanding of glioblastoma. J Neurooncol 2012;108:11–27.
21. Pansuriya TC, van Eijk R, d'Adamo P, van Ruler MA, Kuijjer ML, Oosting J, et al. Somatic mosaic IDH1 and IDH2 mutations are associated with enchondroma and spindle cell hemangioma in Ollier disease and Maffucci syndrome. Nat Genet 2011;43:1256–61.
22. Saha SK, Parachoniak CA, Ghanta KS, Fitamant J, Ross KN, Najem MS, et al. Mutant IDH inhibits HNF-4alpha to block hepatocyte differentiation and promote biliary cancer. Nature 2014;513:110–4.
23. Rohle D, Popovici-Muller J, Palaskas N, Turcan S, Grommes C, Campos C, et al. An inhibitor of mutant IDH1 delays growth and promotes differentiation of glioma cells. Science 2013;340:626–30.

Published OnlineFirst September 11, 2015; DOI: 10.1158/0008-5472.CAN-14-3603

24. Wang F, Travins J, DeLaBarre B, Penard-Lacronique V, Schalm S, Hansen E, et al. Targeted inhibition of mutant IDH2 in leukemia cells induces cellular differentiation. Science 2013;340:622–6.
25. Davis MI, Gross S, Shen M, Straley KS, Pragani R, Lea WA, et al. Biochemical, cellular, and biophysical characterization of a potent inhibitor of mutant isocitrate dehydrogenase IDH1. J Biol Chem 2014;289:13717–25.
26. Chaturvedi A, Araujo Cruz MM, Jyotsana N, Sharma A, Yun H, Gorlich K, et al. Mutant IDH1 promotes leukemogenesis in vivo and can be specifically targeted in human AML. Blood 2013;122:2877–87.
27. Deng G, Shen J, Yin M, McManus J, Mathieu M, Gee P, et al. Selective inhibition of mutant isocitrate dehydrogenase 1 (IDH1) via disruption of a metal binding network by an allosteric small molecule. J Biol Chem 2015;290:762–74
28. Fernandez SL, Russell DW, Hurlin PJ. Development of human gene reporter cell lines using rAAV mediated homologous recombination. Biol Proced Online 2007;9:84–90.
29. Esmaeili M, Hamans BC, Navis AC, van Horssen R, Bathen TF, Gribbestad IS, et al. IDH1 R132H mutation generates a distinct phospholipid metabolite profile in glioma. Cancer Res 2014;74:4898–907.
30. Capper D, Zentgraf H, Balss J, Hartmann C, von Deimling A. Monoclonal antibody specific for IDH1 R132H mutation. Acta Neuropathol 2009; 118:599–601.
31. Chieco P, Jonker A, De Boer BA, Ruijter JM, Van Noorden CJ. Image cytometry: protocols for 2D and 3D quantification in microscopic images. Prog Histochem Cytochem 2013;47:211–333.
32. Shi Q, Karuppagounder SS, Xu H, Pechman D, Chen H, Gibson GE. Responses of the mitochondrial alpha-ketoglutarate dehydrogenase complex to thiamine deficiency may contribute to regional selective vulnerability. Neurochem Int 2007;50:921–31.
33. Franken NA, Rodermond HM, Stap J, Haveman J, van Bree C. Clonogenic assay of cells in vitro. Nat Protoc 2006;1:2315–9.
34. Miller SA, Dykes DD, Polesky HF. A simple salting out procedure for extracting DNA from human nucleated cells. Nucleic Acids Res 1988; 16:1215.
35. Aryee MJ, Jaffe AE, Corrada-Bravo H, Ladd-Acosta C, Feinberg AP, Hansen KD, et al. Minfi: a flexible and comprehensive Bioconductor package for the analysis of Infinium DNA methylation microarrays. Bioinformatics 2014;30:1363–9.
36. Aten JA, Stap J, Krawczyk PM, van Oven CH, Hoebe RA, Essers J, et al. Dynamics of DNA double-strand breaks revealed by clustering of damaged chromosome domains. Science 2004;303:92–5.
37. Gilbert MR, Liu Y, Neltner J, Pu H, Morris A, Sunkara M, et al. Autophagy and oxidative stress in gliomas with IDH1 mutations. Acta Neuropathol 2014;127:221–33.
38. Latini A, Scussiato K, Rosa RB, Llesuy S, Bello-Klein A, Dutra-Filho CS, et al. D-2-hydroxyglutaric acid induces oxidative stress in cerebral cortex of young rats. Eur J Neurosci 2003;17:2017–22.
39. Kolker S, Pawlak V, Ahlemeyer B, Okun JG, Horster F, Mayatepek E, et al. NMDA receptor activation and respiratory chain complex V inhibition contribute to neurodegeneration in d-2-hydroxyglutaric aciduria. Eur J Neurosci 2002;16:21–8.
40. Reitman ZJ, Sinenko SA, Spana EP, Yan H. Genetic dissection of leukemia-associated IDH1 and IDH2 mutants and D-2-hydroxyglutarate in Drosophila. Blood 2015;125:336–45.
41. Koivunen P, Lee S, Duncan CG, Lopez G, Lu G, Ramkissoon S, et al. Transformation by the (R)-enantiomer of 2-hydroxyglutarate linked to EGLN activation. Nature 2012;483:484–8.
42. Grassian AR, Parker SJ, Davidson SM, Divakaruni AS, Green CR, Zhang X, et al. IDH1 mutations alter citric acid cycle metabolism and increase dependence on oxidative mitochondrial metabolism. Cancer Res 2014; 74:3317–31.
43. Cuyas E, Fernandez-Arroyo S, Corominas-Faja B, Rodriguez-Gallego E, Bosch-Barrera J, Martin-Castillo B, et al. Oncometabolic mutation IDH1 R132H confers a metformin-hypersensitive phenotype. Oncotarget 2015; 6:12279–96.
44. Wolf DA. Is reliance on mitochondrial respiration a "chink in the armor" of therapy-resistant cancer? Cancer Cell 2014;26:788–95.
45. Molenaar RJ, Thota S, Nagata Y, Patel B, Clemente M, Hirsh C, et al. Clinical and biological implications of ancestral and non-ancestral IDH1 and IDH2 mutations in myeloid neoplasms. Leukemia 2015 Apr 3. [Epub ahead of print].
46. Peters AL, VanNoorden CJ. Glucose-6-phosphate dehydrogenase deficiency and malaria: cytochemical detection of heterozygous G6PD deficiency in women. J Histochem Cytochem 2009;57:1003–11.
47. Cancer Genome Atlas N. Comprehensive molecular characterization of human colon and rectal cancer. Nature 2012;487:330–7.
48. Ward PS, Patel J, Wise DR, Abdel-Wahab O, Bennett BD, Coller HA, et al. The common feature of leukemia-associated IDH1 and IDH2 mutations is a neomorphic enzyme activity converting alpha-ketoglutarate to 2-hydroxyglutarate. Cancer Cell 2010;17:225–34.
49. Yang B, Zhong C, Peng Y, Lai Z, Ding J. Molecular mechanisms of "off-on switch" of activities of human IDH1 by tumor-associated mutation R132H. Cell Res 2010;20:1188–200.
50. Chan SM, Thomas D, Corces-Zimmerman MR, Xavy S, Rastogi S, Hong WJ, et al. Isocitrate dehydrogenase 1 and 2 mutations induce BCL-2 dependence in acute myeloid leukemia. Nat Med 2015;21:178–84.
51. Kranendijk M, Struys EA, Salomons GS, Van der Knaap MS, Jakobs C. Progress in understanding 2-hydroxyglutaric acidurias. J Inherit Metab Dis 2012;35:571–87.
52. Sasaki M, Knobbe CB, Itsumi M, Elia AJ, Harris IS, Chio II, et al. D-2-hydroxyglutarate produced by mutant IDH1 perturbs collagen maturation and basement membrane function. Genes Dev 2012;26:2038–49.
53. Schumacher T, Bunse L, Pusch S, Sahm F, Wiestler B, Quandt J, et al. A vaccine targeting mutant IDH1 induces antitumour immunity. Nature 2014;512:324–7.
54. Molenaar RJ, van Noorden CJ. Type 2 diabetes and cancer as redox diseases? Lancet 2014;384:853.
55. van Lith SA, Molenaar R, van Noorden CJ, Leenders WP. Tumor cells in search for glutamate: an alternative explanation for increased invasiveness of IDH1 mutant gliomas. Neuro Oncol 2014;16:1669–70.
56. Chen R, Nishimura MC, Kharbanda S, Peale F, Deng Y, Daemen A, et al. Hominoid-specific enzyme GLUD2 promotes growth of IDH1R132H glioma. Proc Natl Acad Sci U S A 2014;111:14217–22.
57. Reitman ZJ, Duncan CG, Poteet E, Winters A, Yan LJ, Gooden DM, et al. Cancer-associated isocitrate dehydrogenase 1 (IDH1) R132H mutation and d-2-hydroxyglutarate stimulate glutamine metabolism under hypoxia. J Biol Chem 2014;289:23318–28.
58. Seltzer MJ, Bennett BD, Joshi AD, Gao P, Thomas AG, Ferraris DV, et al. Inhibition of glutaminase preferentially slows growth of glioma cells with mutant IDH1. Cancer Res 2010;70:8981–7.
59. Elhammali A, Ippolito JE, Collins L, Crowley J, Marasa J, Piwnica-Worms D. A high-throughput fluorimetric assay for 2-hydroxyglutarate identifies Zaprinast as a glutaminase inhibitor. Cancer Discov 2014;4: 828–39.

Cancer Research
The Journal of Cancer Research (1916–1930) | The American Journal of Cancer (1931–1940)

AACR American Association for Cancer Research

Radioprotection of *IDH1*-Mutated Cancer Cells by the IDH1-Mutant Inhibitor AGI-5198

Remco J. Molenaar, Dennis Botman, Myrthe A. Smits, et al.

Cancer Res 2015;75:4790-4802. Published OnlineFirst September 11, 2015.